

MMP: Towards Robust Multi-Modal Learning with Masked Modality Projection

Niki Nezakati¹, Md Kaykobad Reza¹, Ameya Patil², Mashhour Solh², M. Salman Asif¹

¹University of California Riverside ²Amazon

Abstract

Multimodal learning seeks to combine data from multiple input sources to enhance the performance of different downstream tasks. In real-world scenarios, performance can degrade substantially if some input modalities are missing. Existing methods that can handle missing modalities involve custom training or adaptation steps for each input modality combination. These approaches are either tied to specific modalities or become computationally expensive as the number of input modalities increases. In this paper, we propose Masked Modality Projection (MMP), a method designed to train a single model that is robust to any missing modality scenario. We achieve this by randomly masking a subset of modalities during training and learning to project available input modalities to estimate the tokens for the masked modalities. This approach enables the model to effectively learn to leverage the information from the available modalities to compensate for the missing ones, enhancing missing modality robustness. We conduct a series of experiments with various baseline models and datasets to assess the effectiveness of this strategy. Experiments demonstrate that our approach improves robustness to different missing modality scenarios, outperforming existing methods designed for missing modalities or specific modality combinations.

1 Introduction

Multimodal learning (MML) (Baltrušaitis, Ahuja, and Morency 2018; Xu, Zhu, and Clifton 2023) leverages information from multiple input sources to perform better on the underlying task. Incorporating knowledge from diverse input sources has proven to be very effective in enhancing model performance (Huang et al. 2021; Lu 2024). Since these models are generally trained on all input modalities, they rely heavily on the presence of all modalities to perform optimally during test time. In the real-world scenarios, any subset of the modalities can be missing due to sensor malfunction, privacy concerns, or data acquisition constraints. Recent studies have shown that multimodal models show significant performance drop when a subset of input modalities is missing (Ma et al. 2022; Lee et al. 2023). In this paper, we investigate the missing modality issue during test time and show that a single model trained in a robust manner can outperform existing baseline methods in different missing modality scenarios.

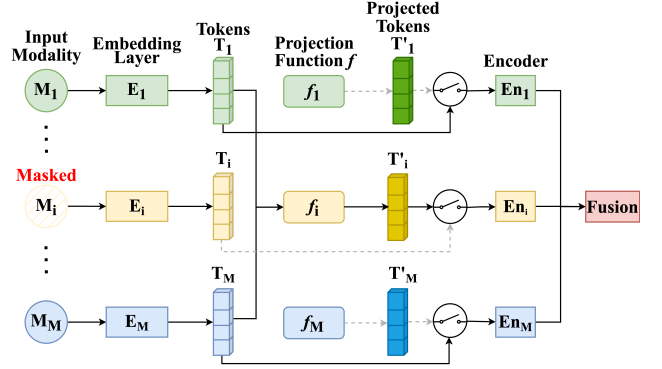


Figure 1: Architecture of the proposed MMP approach for training a single multimodal model that is robust to missing modalities. Input modalities are passed through embedding layers, generating tokens. For a masked modality i , a projection function utilizes the tokens from the available modalities to generate projected tokens. These projected tokens are then passed to the masked modality branch.

A number of approaches has been proposed to enhance missing modality robustness for different multimodal tasks. Some of these approaches include utilizing a robust training approach (Neverova et al. 2015; Hussen Abdelaziz et al. 2020), modality masking (Bachmann et al. 2022; Shin, Lee, and Kweon 2023), or knowledge distillation (Tarvainen and Valpola 2017; Maheshwari, Liu, and Kira 2024; Wu et al. 2024) during training. These approaches force the model to perform better with available modalities either by masking inputs or from the help of a teacher model. Prompting-based methods learn to compensate for the missing modalities with learnable prompts (Lee et al. 2023; Jang, Wang, and Kim 2024); however, they need to learn one set of prompts for each missing modality scenarios, which scales poorly as the number of input modalities increase. Missing modality imputation is another approach where generative networks like generative adversarial network (GAN) (Yu et al. 2018; Sharma and Hamarneh 2019) and variational autoencoder (VAE) (Dorent et al. 2019) are used to generate missing modalities from available modalities. Training such generative networks to impute missing modality adds extra overhead to the overall process.

In this paper, we propose **Masked Modality Projection (MMP)**, a method for training a single multimodal model that is robust to any missing modality scenario. Our approach leverages available modalities to compensate for the missing ones. In particular, we mask out a subset of modalities during training and utilize available modalities to predict the tokens for the masked ones. As illustrated in Figure 1, our approach consists of two main stages: (1) modality masking: where a subset of modalities is masked out during training; and (2) modality projection: where available modalities are used to predict the tokens of the masked modalities, referred to as projected tokens. Additionally, we use alignment loss to align the projected tokens and the actual tokens during training. During inference, the projected tokens are used to substitute for the missing modalities.

Our proposed MMP method can be integrated into any existing multimodal architecture. Moreover, we do not need to train or adapt the model for each missing modality scenario. Experimental results demonstrate that models trained with MMP show significant performance improvement in different missing modality scenarios. We conducted extensive experiments on three baseline models and five datasets, covering three tasks (Section 4). The results show that our method significantly improves performance when some modalities are entirely missing (compared to existing methods), while also maintaining competitive performance when all modalities are available. Performance of the MMP approach is also comparable or better than the models that are exclusively trained for each input modality combination.

Our main contributions can be summarized as follows.

- Masked modality projection (MMP) is a novel approach to predict missing modality tokens from available modalities and enhance robustness to missing modalities.
- MMP provides significantly improved performance with missing modalities compared to models trained with all modalities. The performance is comparable or better than the networks trained for specific modality combinations.
- MMP requires minimal change in the network, which makes it versatile and adaptable across various multimodal tasks, datasets, and models (as demonstrated by our experiments).

2 Related Work

Robust model design is one approach to perform well on missing modality scenarios. Wang et al. (2023) designed a model to learn modality specific and modality shared features and impute missing modality from available ones. On the other hand, Shin, Lee, and Kweon (2023) designed a robust framework based on modality masking and knowledge distillation for RGB-Thermal segmentation. Wang et al. (2022) proposed a method to dynamically detect and replace uninformative tokens with informative tokens. Choi and Lee (2019); Fan et al. (2023); Lin et al. (2023) designed a robust fusion strategies to enhance model robustness in different missing modality situations. For MRI missing modality task, Karimijafarbigloo et al. (2024) proposed a Transformer-based approach with adopted co-training strategy. However, these models and fusion strategies are gen-

erally designed for a specific tasks. So, it is non-trivial to generalize them for other multimodal tasks.

Robust training approach can make models robust to missing modalities. Modality dropout augmentation has been applied by Neverova et al. (2015) for multimodal gesture recognition and Hussen Abdelaziz et al. (2020) for generating 3D facial animation. Modality masking based approaches also gained popularity. Shin, Lee, and Kweon (2023) used complementary random masking and Fan et al. (2023) used partial modality masking for training robust models. Bachmann et al. (2022) utilized masked autoencoders, Ma et al. (2022) utilized masked cross attention and Hazarika et al. (2022) used modality perturbation to make the underlying models robust to missing and corrupted modalities. Though these approaches improve model robustness in missing modality scenarios, they can not compensate the performance drop completely.

Model adaptation is another approach to make models robust to missing scenarios. Lee et al. (2023) trained one set of learnable prompts for each modality combination and used those learned prompts when modalities got missing during test time. A followup study by Jang, Wang, and Kim (2024) showed that learning one set of prompts for each input modality is sufficient for comparable performance. Reza, Prater-Bennette, and Asif (2023) utilized parameter efficient adaptation to build a generic framework to make existing models robust. They validated the effectiveness of their framework on a number of multimodal tasks. The main disadvantage of these approaches is that they require one set of learnable parameters per modality combination.

Generation and knowledge distillation based approaches are also used to enhance model robustness. GAN based generative models were used by Yu et al. (2018), Sharma and Hamarneh (2019), and Zhang et al. (2024). Dorent et al. (2019) used variational autoencoders to generate missing modality. Qu et al. (2024) introduced a local diffusion shared-specific autoencoder to handle missing modality issue in image classification. Studies by Woo et al. (2023) proposed ActionMAE to generate missing feature vectors for robust action recognition. Knowledge distillation also showed great promise in a number of tasks. Shin, Lee, and Kweon (2023) and Maheshwari, Liu, and Kira (2024) utilized knowledge distillation for multimodal segmentation tasks. Wu et al. (2024) used a teacher-student distillation model to combine partially available visual information with auditory information. Wei, Luo, and Luo (2023) presented a framework that uses a teacher network to transfer comprehensive multimodal information for improving multimodal learning with missing data. Apart from these approaches, policy learning (Ma et al. 2022), Bayesian meta-learning (Ma et al. 2021) and weight-space ensembling (Wortsman et al. 2022) are also utilized for missing modality robustness. The main drawback of these approaches is that they need to train/utilize another model to generate missing modality or distill knowledge.

In this paper, our goal is to train a single model that is robust to any missing modality scenario. Our method utilizes available input modalities to generate the tokens for the

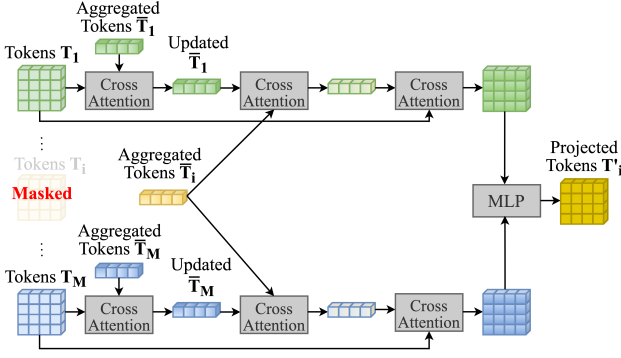


Figure 2: Visualization of the modality projection approach. Available modality tokens are processed through cross-attention to update their aggregated tokens. These aggregated tokens are combined with those of the masked modality through another cross-attention step. The resulting cross-modal relationships are used to attend to the actual tokens of the available modalities. The final output tokens are passed through an MLP to generate the projected tokens of the masked modality.

missing modalities. The model is trained end-to-end without the need for tuning or adapting it for any specific modality combination.

3 Method

In this section, we introduce Masked Modality Projection (MMP), a novel approach for training a single multimodal model that is robust to missing modalities. In this method, a subset of modalities is randomly masked out during each training iteration. To address the absence of these modalities, we introduce projection functions that learn to map tokens from the available modalities to the missing modality tokens, which we refer to as projected tokens. These projected tokens are aligned with the actual tokens using an alignment loss objective. Finally, the projected tokens are passed to the corresponding branch for the masked modality.

3.1 Modality Masking

Modality masking is a key component of our MMP approach. As discussed in Section 2, modality dropout augmentation, which randomly zeros out modalities, has shown robustness to missing modalities. We extend this idea by masking out all the tokens of a random subset of modalities during each training iteration. Instead of feeding zeros, we use available modalities to predict the tokens for the masked modalities. Specifically, at each iteration, a random subset of modalities are selected to be masked (i.e., they are not fed to the model). Our goal is to train the model to predict the tokens of the masked modalities using the available ones.

3.2 Modality Projection

We propose a modality projection approach for masked modality i , as illustrated in Figure 2. Suppose we have M distinct modalities given as input. The embedding layers generate tokens from each input modality as

$$\mathbf{T}_i = \text{EmbeddingLayer}(\mathbf{I}_i), \quad (1)$$

where \mathbf{I}_i represents input modality $i \in \{1, 2, \dots, M\}$ and $\mathbf{T}_i \in \mathbb{R}^{N \times d}$ denotes tokens for modality i , N is the number of tokens, and d is the embedding dimension. For simplicity, here we assume N and d to be the same across modalities. We will discuss how our method can be extended to handle cases with varying numbers of tokens and embedding dimensions among modalities in Section 3.3.

We introduce the projection function f_i to predict the tokens of the masked modality i . This process begins by utilizing aggregated tokens. Inspired by Mo and Morgado (2024), aggregated tokens summarize the modality information into a compact representation; therefore, reducing the computational and storage complexity associated with numerous modality tokens. For each modality i , we use eight aggregated tokens $\bar{\mathbf{T}}_i$, initialized randomly as learnable parameters. When modality j is available during an iteration, its aggregated tokens $\bar{\mathbf{T}}_j$ are updated by attending to the actual modality tokens \mathbf{T}_j using multi-head cross-attention. This process is represented as

$$\begin{aligned} \bar{\mathbf{T}}_j &= \text{CrossAttention}(\bar{\mathbf{T}}_j, \mathbf{T}_j \mid j \in \mathcal{A}), \\ &= \text{softmax} \left(\frac{\bar{\mathbf{T}}_j \mathbf{W}_q \mathbf{W}_k^\top \mathbf{T}_j^\top}{\sqrt{d}} \right) \mathbf{T}_j \mathbf{W}_v, \end{aligned} \quad (2)$$

where $\mathbf{T}_j \in \mathbb{R}^{N \times d}$ and $\bar{\mathbf{T}}_j \in \mathbb{R}^{8 \times d}$ denote tokens and aggregated tokens of modality j , respectively, and \mathcal{A} is the set of available modalities.

\mathbf{W}_q , \mathbf{W}_k , and \mathbf{W}_v are learnable weight matrices for the query, key, and value projections, respectively. The aggregated tokens are only updated when a modality is available; if modality i is masked at an iteration, its aggregated tokens $\bar{\mathbf{T}}_i$ are left unchanged.

When dealing with missing modalities, for each modality i that is missing (masked during training), cross-attention is performed between the aggregated tokens of the missing modality and the aggregated tokens of each available modality separately. This step captures the relationships between the missing modality and each available modality, allowing the model to approximate the missing modality information based on available data. Specifically

$$\mathbf{X}_{ij} = \text{CrossAttention}(\bar{\mathbf{T}}_i, \bar{\mathbf{T}}_j), \quad (3)$$

where $\bar{\mathbf{T}}_i, \bar{\mathbf{T}}_j$ are the aggregated tokens of missing modality i , available modality j , respectively. \mathbf{X}_{ij} represents the attended tokens for available modality j in relation to missing modality i .

We then utilize \mathbf{X}_{ij} in cross-attention with the original tokens \mathbf{T}_j of available modality j to ensure that the relational information is integrated with the specific features of each available modality. The refinement process is expressed as

$$\mathbf{T}_{\text{attended}_j} = \text{CrossAttention}(\mathbf{T}_j, \mathbf{X}_{ij}), \quad (4)$$

where $\mathbf{T}_{\text{attended}_j}$ denotes the refined attended tokens for available modality j . The refined attended tokens are then concatenated for each available modality j

$$\mathbf{T}_{\text{available}} = \text{Concat}(\{\mathbf{T}_{\text{attended}_j} \mid j \in \mathcal{A}\}), \quad (5)$$

where \mathcal{A} denotes the set of available modalities. The concatenated tokens $\mathbf{T}_{\text{available}}$ are then fed into a multi-layer perceptron (MLP) to produce the projected tokens \mathbf{T}'_i for the missing modality i as

$$\mathbf{T}'_i = \text{MLP}(\mathbf{T}_{\text{available}}). \quad (6)$$

The missing modality tokens are replaced with their corresponding projected tokens \mathbf{T}'_i and passed to their respective branch in the network.

3.3 Token and Dimension Variability

Our method can also be applied in cases where the number of tokens N or the embedding dimension d differs across modalities. To address differences in embedding dimensions, we apply a linear layer at the beginning of the projection process to map tokens from each modality to a common embedding dimension. For cases where the number of tokens varies, we incorporate a linear layer within the MLP module to align the token count of the projected tokens \mathbf{T}'_i with that of the missing modality i .

3.4 Alignment Loss Objective

To minimize the discrepancy between the projected and real tokens, we use an alignment loss objective to ensure that the projected tokens closely match their corresponding real tokens. If N_{masked} denotes the number of masked modalities at an iteration, the alignment loss is computed as

$$\mathcal{L}_{\text{alignment}} = \frac{1}{N_{\text{masked}}} \sum_{i \in \text{masked}} \mathcal{L}_{\text{alignment}_i}(\mathbf{T}'_i, \mathbf{T}_i), \quad (7)$$

where $\mathcal{L}_{\text{alignment}_i}$ represents the Smooth L1 loss between the real tokens \mathbf{T}_i and the projected tokens \mathbf{T}'_i . To incorporate the alignment loss into the overall optimization, we add $\mathcal{L}_{\text{alignment}}$ to the network's primary loss function as

$$\mathcal{L}_{\text{total}} = \mathcal{L}_{\text{task}} + \mathcal{L}_{\text{alignment}} \quad (8)$$

where $\mathcal{L}_{\text{task}}$ represents the primary task-specific loss of the network.

4 Experiments and Results

In this section, we provide a comprehensive evaluation of our proposed method through detailed experiments on multimodal segmentation and classification tasks across five datasets. We compare our approach with established baseline methods that address missing modalities to assess its effectiveness and generalizability.

4.1 Datasets

MCubeS dataset (Liang et al. 2022) contains 500 sets of images split into training, validation, and test sets containing 302, 96, and 102 sets of images respectively. It has 4 input modalities and per-pixel annotations for 20 material classes. **NYUDv2 dataset** (Silberman et al. 2012) contains 1,449 aligned RGB-Depth image pairs, split into 795 for training and 654 for testing. Each images is 640×480 pixels and has annotation for 40 classes.

FMB dataset (Liu et al. 2023) has 1,500 calibrated RGB-Infrared image pairs, with 1,220 for training and 280 for testing. It includes diverse scenes across various lighting and weather conditions, and offers per-pixel ground truth annotations for 14 classes.

UPMC Food-101 dataset (Wang et al. 2015) is a multimodal classification dataset containing image and text as input modalities. The dataset contains 90,704 image-text pairs divided into train, validation and test sets, and 101 food categories.

CMU-MOSI dataset (Zadeh et al. 2016) is widely used for multimodal sentiment analysis and includes audio, visual, and text modalities. It contains a total of 2,199 samples, which are divided into training, validation, and test sets with 1,284, 229, and 686 samples respectively.

Complete details about each dataset are added in the supplementary materials of this paper.

4.2 Implementation Details

We use CMNeXt (Zhang et al. 2023) as the base model for multimodal segmentation, ViLT (Kim, Son, and Kim 2021) for multimodal classification, and multimodal transformer (Tsai et al. 2019) for multimodal sentiment analysis task. To evaluate missing modality performance, available modalities are provided while missing ones are set to zero for visual and audio data, and to empty strings for texts. For multimodal segmentation, we use a learning rate of 6×10^{-5} with a polynomial scheduler, and apply OHEM cross-entropy loss for the FMB and MCubeS datasets, and cross-entropy loss for NYUDv2. We utilize AdamW (Loshchilov and Hutter 2019), with $\epsilon = 10^{-8}$ and a weight decay of 0.01. For this task, we utilize the CMNeXt model pre-trained with modality dropout augmentation. We set the batch size to 4, and train the model for 500 epochs on MCubeS and NYUDv2 dataset. For the FMB dataset, we use a batch size of 2 and train for 120 epochs. For multimodal classification, we set the learning rate to 10^{-5} , and utilize polynomial learning rate scheduler. We use cross-entropy loss, and AdamW optimizer with the same configuration as the multimodal segmentation task. Batch size is 16, and we train the model for 20 epochs. The remaining configurations of this task are the default settings from (Lee et al. 2023). For multimodal sentiment analysis we used the default settings from (Yu et al. 2021). Further implementation details are added in the supplementary materials of this paper.

4.3 Results on Multimodal Segmentation

We present a comparison of multimodal segmentation performance across the MCubeS, NYUDv2, and FMB datasets in Table 1. All experiments were conducted using the CMNeXt (Zhang et al. 2023) model to ensure consistency and fairness. **Pretrained** column indicates the performance when we train the model without dropout augmentation and test the performance on different missing modality scenarios. **Modality dropout** column indicates the performance when we use dropout augmentation while training the model. **MMP** column indicates the performance when we utilize our modality projection approach to generate tokens for the missing modalities.

Dataset	Input Modalities	Missing Modalities	Pretrained	Modality Dropout	MMP (ours)
MCubeS	RGB-A-D-N	-	51.54	48.56	48.95
	A-D-N	RGB	1.45	33.88	38.57
	A-D	RGB-N	0.93	33.15	37.74
	A	RGB-D-N	1.13	26.3	31.31
NYUDv2	RGB-Depth	-	56.30	51.12	53.81
	RGB	Depth	51.05	48.80	52.04
	Depth	RGB	6.01	29.79	41.08
FMB	RGB-Thermal	-	62.68	54.11	60.03
	RGB	Thermal	22.2	48.32	55.83
	Thermal	RGB	23.35	39.66	51.73

Table 1: Performance comparison (mIoU) of the pretrained model, modality dropout training, and MMP. Input and missing modalities columns indicate available and missing modalities during inference. A, D and N denote angle of linear polarization, degree of linear polarization, and near-infrared, respectively.

Methods	Backbone	RGB	Depth	Avg.
AsymFusion (2020b)	ResNet-101	46.50	34.30	40.40
CEN (2020a)	ResNet-101	39.59	19.32	29.46
TokenFusion (2022)	MiT-B3	49.32	36.84	43.08
Reza et. al. (2023)	MiT-B4	52.82	36.72	<u>44.77</u>
MMANet (2023)	ResNet-50	44.93	42.75	43.84
HeMIS (2016)	ResNet-50	33.23	31.23	32.23
CMNeXt (2023)	MiT-B4	51.19	5.26	28.23
RFNet (2021)	ResNet-50	42.89	40.76	41.82
MMP (Ours)	MiT-B4	<u>52.04</u>	<u>41.08</u>	46.56

Table 2: Performance (mIoU) comparison with existing methods on NYUDv2 dataset. RGB, Depth and Avg. columns report RGB only, Depth only and average performance respectively. Best and second-best results are shown as **bold** and underlined, respectively.

Our findings indicate that the pretrained model experiences a notable performance drop when modalities get missing during test time. Although modality dropout improves performance in missing modality scenarios, it does not fully mitigate the performance drop. In contrast, our MMP approach utilizes the available modalities to generate tokens for missing ones, further enhancing robustness and performance across all datasets. Specifically, our MMP approach outperforms both the pretrained model and modality dropout in every missing modality scenario, demonstrating its effectiveness in compensating for missing modalities. The slightly reduced performance of the MMP approach when all modalities are available is due to the base model being pretrained with modality dropout, which has lower performance when all modalities are present.

We report experimental results for different baseline methods on NYUDv2 in Table 2. Compared to other methods, our MMP approach achieves superior average performance. When Depth is missing, MMP ranks second to Reza et. al. (2023), which learns adaptable layers for different modality combinations. The performance difference is minimal (-0.78%), and MMP outperforms this method in both average (+1.79%) and RGB-missing (+4.36%) scenarios.

Available Modality	ViLT	Missing Prompts (2023)	MMP
Image	Text	Attention	Input
100%	100%	92.71 [†]	92.71
100%	30%	66.29	72.57
100%	0%	23.70 [†]	67.70
65%	65%	69.25	78.09
30%	100%	76.66	86.05
0%	100%	82.65 [†]	85.30

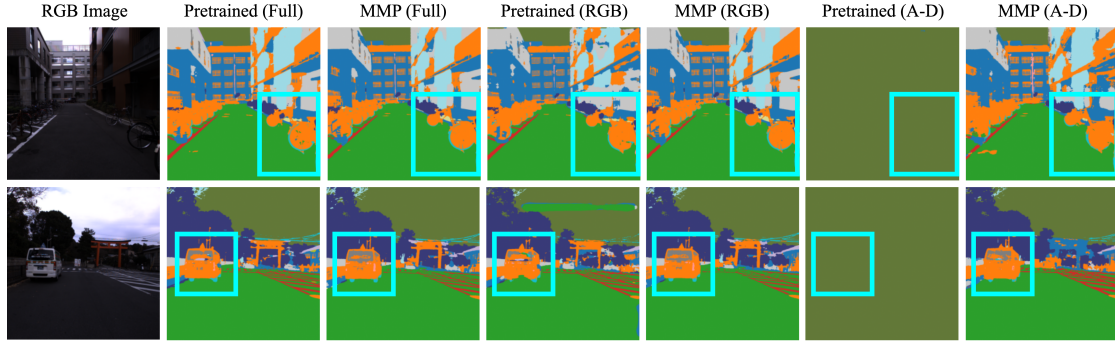
Table 3: Performance (accuracy) comparison for multimodal classification on UPMC Food-101 dataset. Available modality column shows the percentage of image and text modality available during inference. † indicates that the results were generated using the available code from the authors.

This demonstrates that MMP has matched or exceeded the performance of this method while eliminating the computational overhead of adapting the model separately for each modality combination. When RGB is missing, MMP is the second-best to MMANet (2023). Notably, MMANet relies on a teacher model trained with all modalities, yet our MMP approach achieves better performance in other cases without the added complexity of training a separate teacher model.

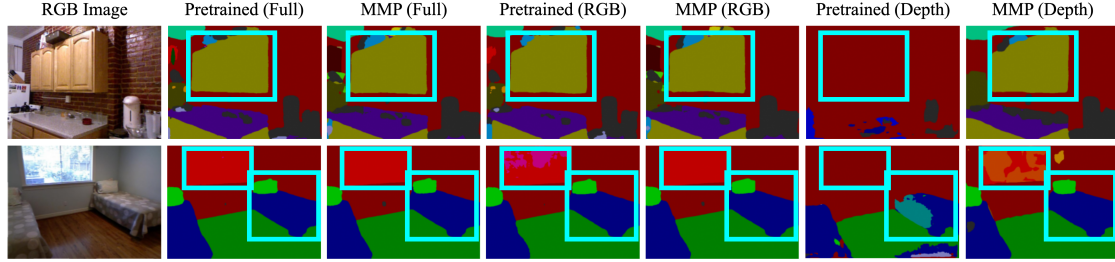
4.4 Visualization of Predictions

To better demonstrate the impact of our approach, we visualize the predicted segmentation maps from the pretrained CMNeXt model and our MMP approach in Figure 3. For each dataset, we show the RGB image and predictions from the pretrained model and MMP approach with different available modalities (available modality names are shown in parentheses above each image). We highlight the impact of presence of the RGB modality due to its greater emphasis in the CMNeXt model’s design.

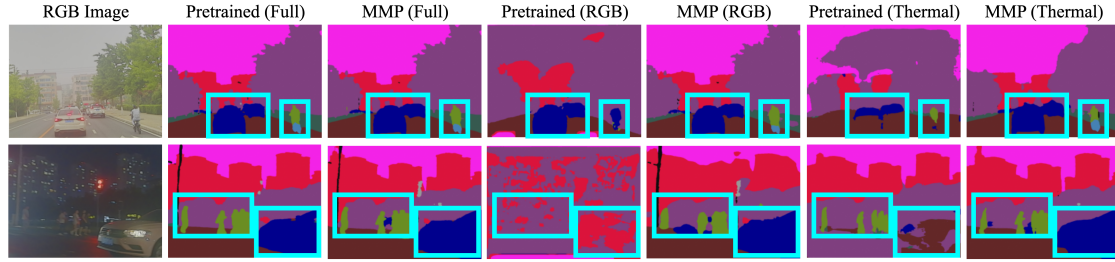
In Figure 3a, we observe that the pretrained model struggles to detect the bikes and cars when the Angle of Linear Polarization (AoLP), Degree of Linear Polarization (DoLP), and Near-Infrared (NIR) modalities are missing. When RGB is missing along with NIR, and only AoLP and



(a) Visualization of multimodal material segmentation predictions on MCubeS dataset



(b) Visualization of multimodal semantic segmentation predictions on NYUDv2 dataset



(c) Visualization of multimodal semantic segmentation predictions on FMB dataset

Figure 3: Visualization of predicted segmentation maps for the Pretrained (CMNeXt) model and our MMP approach. Title above each image indicates the method name (available modalities). Blue boxes mark the areas where the differences are more prominent. A and D denote angle and degree of linear polarization, respectively.

DoLP are available, the pretrained model fails to perform any segmentation. In contrast, our MMP approach successfully detects the bikes and cars even with missing modalities. On NYUDv2 dataset, as shown in Figure 3b, MMP demonstrates superior accuracy in detecting kitchen cabinets, counter-tops, windows, and beds compared to the pretrained model with missing modalities. In Figure 3c, the pretrained model fails to detect the car, bicyclist, and humans when modalities are missing. However, our MMP approach successfully detects all these objects in every scenario. In all examples, our MMP predictions are either better or comparable to the pretrained model with all modalities available. When modalities are missing, MMP consistently outperforms the pretrained model and closely matches the performance achieved with full input.

4.5 Results on Multimodal Classification

We further evaluate the effectiveness of our approach by performing a comparison against the missing-aware prompts method (Lee et al. 2023) using the UPMC Food-101 (Wang et al. 2015) dataset. Experiments on multimodal classification task were conducted on ViLT (Kim, Son, and Kim 2021) as the base model. The results are detailed in Table 3. Our MMP outperforms the prompting-based methods in most scenarios, achieving better overall results. Our performance shows a slight decrease in two cases, 0.21% lower when 70% of text is missing, and 2.04% lower when no text is available. This is because prompting-based methods learn one set of prompts for each missing modality scenario and thus outperform MMP in certain modality combinations. Notably, our approach maintains strong performance across various missing modality scenarios without requiring train-

Method	Backbone	Text-Visual-Audio		Visual-Audio		Audio		Average	
		Acc	F1	Acc	F1	Acc	F1	Acc	F1
MuT (2019)	Transformer	<u>79.57</u>	<u>79.67</u>	48.93	41.95	48.31	40.98	58.93	54.20
TFN (2017)	LSTM	73.90	73.40	42.23	25.07	42.23	25.07	52.78	41.18
LMF (2018)	LSTM	76.40	75.70	43.29	27.61	42.23	25.07	53.97	42.79
Reza et. al. (2023)	Transformer	<u>79.57</u>	<u>79.67</u>	55.49	53.96	<u>50.00</u>	<u>46.71</u>	61.68	60.11
MMP (Ours)	Transformer	80.03	80.04	<u>54.73</u>	<u>52.24</u>	55.03	53.98	63.26	62.08

Table 4: Performance (binary accuracy and F1 score) comparison with existing methods for multimodal sentiment analysis on CMU-MOSI dataset. Column names indicate available modalities. Best and second-best results are shown as **bold** and underlined, respectively.

Methods	RGB-Depth	RGB	Depth	Average
Dropout	51.12	48.80	29.79	43.23
Dropout + LP	51.31	51.08	35.48	45.95
Dropout + LP + Align	52.84	50.73	40.60	48.05
Dropout + CA + Align	53.81	52.04	41.08	48.97

Table 5: Ablation studies on NYUDv2 dataset. Modality dropout shows significant performance drop when RGB is missing. Performance increases as we apply linear projection (LP). Adding alignment loss (Align) improves performance further. Finally, replacing linear projection with cross attention (CA) shows overall best performance.

ing for every possible modality combination.

4.6 Results on Multimodal Sentiment Analysis

We evaluated our approach on the CMU-MOSI dataset (Zadeh et al. 2016) for multimodal sentiment analysis, with results presented in Table 4. We utilized the multimodal transformer (MuT) (Tsai et al. 2019) as the base model for this task. Our findings indicate that when the text modality is present, missing audio, video, or both has little impact on performance, as noted in Hazarika et al. (2022) and Reza, Prater-Bennette, and Asif (2023). However, performance drops significantly without the text modality. Our MMP approach effectively compensates for this, providing a substantial improvement over the base MuT model. Specifically, we observe a 5.8% improvement in accuracy and a 10.29% increase in F1 score when text is missing. When only the audio modality is available, and both text and visual modalities are absent, MMP achieves larger improvements of 6.72% in accuracy and 13% in F1 score. MMP outperforms existing methods in both accuracy and F1 score across all scenarios, except when only text is missing, where it ranks second. The performance difference between MMP and the best-performing method (Reza et. al. (2023)) in this case is minimal. However, MMP surpasses this method by a large margin in other scenarios, resulting in higher average accuracy and F1 scores overall.

4.7 Ablation Studies

To further investigate the contributions of various components in our proposed MMP approach, we conducted an ablation study on the NYUDv2 dataset. Table 5 summarizes the results. We began with evaluating the performance of

modality dropout, which serves as a baseline for comparison. Modality dropout shows significant performance drop when RGB is missing. Then we add a single linear layer as the projection function (LP) with modality dropout, to predict the tokens of the dropped modality using a linear combination of the available ones. This approach led to performance improvements across all scenarios. Next, we utilized an alignment loss (Align) objective with the linear projection and modality dropout. We observed further performance improvement in all cases, particularly when RGB was missing. Finally, we replaced the single linear layer with MMP’s cross-attention based (CA) projection approach, combined with modality dropout and alignment loss. This final configuration achieved the highest performance among all the tested setups. Based on these experimental results, we argue that each component in our MMP module plays a critical role in enhancing the overall model performance in different missing modality scenarios.

5 Conclusion

In this paper, we introduced Masked Modality Projection (MMP), a novel approach designed to enhance missing modality robustness of multimodal models. Our approach eliminates the need for training or adapting models for specific missing modality scenarios. We demonstrate that a single model can effectively handle any missing modality scenario and outperform current baselines. Thus it reduces both time and computational overhead. Experimental results across several baseline models and datasets validate that MMP significantly improves performance and robustness compared to existing baseline methods. Future work will focus on further refining MMP and exploring its applicability to other multimodal tasks and datasets. We believe that MMP offers an efficient and effective solution to the challenge of missing modalities.

Acknowledgment: This work is supported in part by AFOSR award FA9550-21-1-0330 and an Amazon Gift award. This work used Indiana Jetstream2 through allocation CIS220128 from the ACCESS program supported by NSF grants 2138259, 2138286, 2138307, 2137603, and 2138296.

References

- Bachmann, R.; Mizrahi, D.; Atanov, A.; and Zamir, A. 2022. MultiMAE: Multi-modal Multi-task Masked Autoencoders. In *European Conference on Computer Vision*.
- Baltrušaitis, T.; Ahuja, C.; and Morency, L.-P. 2018. Multimodal machine learning: A survey and taxonomy. *IEEE Transactions on Pattern Analysis and Machine Intelligence*, 41(2): 423–443.
- Bossard, L.; Guillaumin, M.; and Van Gool, L. 2014. Food-101—mining discriminative components with random forests. In *Computer vision—ECCV 2014: 13th European conference, zurich, Switzerland, September 6–12, 2014, proceedings, part VI 13*, 446–461. Springer.
- Chen, X.; Lin, K.-Y.; Wang, J.; Wu, W.; Qian, C.; Li, H.; and Zeng, G. 2020. Bi-directional cross-modality feature propagation with separation-and-aggregation gate for RGB-D semantic segmentation. In *European conference on computer vision*, 561–577. Springer.
- Choi, J.-H.; and Lee, J.-S. 2019. EmbraceNet: A robust deep learning architecture for multimodal classification. *Information Fusion*, 51: 259–270.
- Ding, Y.; Yu, X.; and Yang, Y. 2021. RFNet: Region-aware fusion network for incomplete multi-modal brain tumor segmentation. In *Proceedings of the IEEE/CVF international conference on computer vision*, 3975–3984.
- Dorent, R.; Joutard, S.; Modat, M.; Ourselin, S.; and Vercauteren, T. 2019. Hetero-modal variational encoder-decoder for joint modality completion and segmentation. In *Medical Image Computing and Computer Assisted Intervention—MICCAI 2019: 22nd International Conference, Shenzhen, China, October 13–17, 2019, Proceedings, Part II 22*, 74–82. Springer.
- Fan, S.; Wang, Z.; Wang, Y.; and Liu, J. 2023. SpiderMesh: Spatial-aware Demand-guided Recursive Meshing for RGB-T Semantic Segmentation. *arXiv:2303.08692*.
- Havaei, M.; Guizard, N.; Chapados, N.; and Bengio, Y. 2016. Hemis: Hetero-modal image segmentation. In *Medical Image Computing and Computer-Assisted Intervention—MICCAI 2016: 19th International Conference, Athens, Greece, October 17–21, 2016, Proceedings, Part II 19*, 469–477. Springer.
- Hazarika, D.; Li, Y.; Cheng, B.; Zhao, S.; Zimmermann, R.; and Poria, S. 2022. Analyzing Modality Robustness in Multimodal Sentiment Analysis. In *Proceedings of the 2022 Conference of the North American Chapter of the Association for Computational Linguistics: Human Language Technologies*, 685–696. Association for Computational Linguistics.
- Huang, Y.; Du, C.; Xue, Z.; Chen, X.; Zhao, H.; and Huang, L. 2021. What makes multi-modal learning better than single (provably). *Advances in Neural Information Processing Systems*, 34: 10944–10956.
- Hussen Abdelaziz, A.; Theobald, B.-J.; Dixon, P.; Knothe, R.; Apostoloff, N.; and Kajareker, S. 2020. Modality dropout for improved performance-driven talking faces. In *Proceedings of the 2020 International Conference on Multi-modal Interaction*, 378–386.
- Jang, J.; Wang, Y.; and Kim, C. 2024. Towards Robust Multimodal Prompting with Missing Modalities. In *ICASSP 2024-2024 IEEE International Conference on Acoustics, Speech and Signal Processing (ICASSP)*, 8070–8074. IEEE.
- Karimijafarbigloo, S.; Azad, R.; Kazerouni, A.; Ebadollahi, S.; and Merhof, D. 2024. Mmcformer: Missing modality compensation transformer for brain tumor segmentation. In *Medical Imaging with Deep Learning*, 1144–1162. PMLR.
- Kim, W.; Son, B.; and Kim, I. 2021. Vilt: Vision-and-language transformer without convolution or region supervision. In *International conference on machine learning*, 5583–5594. PMLR.
- Lee, Y.-L.; Tsai, Y.-H.; Chiu, W.-C.; and Lee, C.-Y. 2023. Multimodal prompting with missing modalities for visual recognition. In *Proceedings of the IEEE/CVF Conference on Computer Vision and Pattern Recognition*, 14943–14952.
- Liang, Y.; Wakaki, R.; Nobuhara, S.; and Nishino, K. 2022. Multimodal Material Segmentation. In *Proceedings of the IEEE/CVF Conference on Computer Vision and Pattern Recognition (CVPR)*, 19800–19808.
- Lin, B.; Lin, Z.; Guo, Y.; Zhang, Y.; Zou, J.; and Fan, S. 2023. Variational Probabilistic Fusion Network for RGB-T Semantic Segmentation. *arXiv preprint arXiv:2307.08536*.
- Liu, J.; Liu, Z.; Wu, G.; Ma, L.; Liu, R.; Zhong, W.; Luo, Z.; and Fan, X. 2023. Multi-interactive feature learning and a full-time multi-modality benchmark for image fusion and segmentation. In *Proceedings of the IEEE/CVF international conference on computer vision*, 8115–8124.
- Liu, Z.; Shen, Y.; Lakshminarasimhan, V. B.; Liang, P. P.; Bagher Zadeh, A.; and Morency, L.-P. 2018. Efficient Low-rank Multimodal Fusion With Modality-Specific Factors. In *Proceedings of the 56th Annual Meeting of the Association for Computational Linguistics (Volume 1: Long Papers)*, 2247–2256. Association for Computational Linguistics.
- Loshchilov, I.; and Hutter, F. 2019. Decoupled Weight Decay Regularization. In *International Conference on Learning Representations*.
- Lu, Z. 2024. A theory of multimodal learning. *Advances in Neural Information Processing Systems*, 36.
- Ma, M.; Ren, J.; Zhao, L.; Testuggine, D.; and Peng, X. 2022. Are multimodal transformers robust to missing modality? In *Proceedings of the IEEE/CVF Conference on Computer Vision and Pattern Recognition*, 18177–18186.
- Ma, M.; Ren, J.; Zhao, L.; Tulyakov, S.; Wu, C.; and Peng, X. 2021. Smil: Multimodal learning with severely missing modality. In *Proceedings of the AAAI Conference on Artificial Intelligence*, volume 35, 2302–2310.
- Maheshwari, H.; Liu, Y.-C.; and Kira, Z. 2024. Missing modality robustness in semi-supervised multi-modal semantic segmentation. In *Proceedings of the IEEE/CVF Winter Conference on Applications of Computer Vision*, 1009–1019. IEEE Computer Society.
- Mo, S.; and Morgado, P. 2024. Unveiling the Power of Audio-Visual Early Fusion Transformers with Dense Interactions through Masked Modeling. In *Proceedings of the IEEE/CVF Conference on Computer Vision and Pattern Recognition*, 27186–27196.

- Neverova, N.; Wolf, C.; Taylor, G.; and Nebout, F. 2015. ModDrop: Adaptive multi-modal gesture recognition. *IEEE Transactions on Pattern Analysis and Machine Intelligence*, 38(8): 1692–1706.
- Qu, J.; Yang, Y.; Dong, W.; and Yang, Y. 2024. LDS2AE: Local Diffusion Shared-Specific Autoencoder for Multi-modal Remote Sensing Image Classification with Arbitrary Missing Modalities. In *Proceedings of the AAAI Conference on Artificial Intelligence*, volume 38, 14731–14739.
- Reza, M. K.; Prater-Bennette, A.; and Asif, M. S. 2023. Robust Multimodal Learning with Missing Modalities via Parameter-Efficient Adaptation. *arXiv preprint arXiv:2310.03986*.
- Sharma, A.; and Hamarneh, G. 2019. Missing MRI pulse sequence synthesis using multi-modal generative adversarial network. *IEEE Transactions on Medical Imaging*, 39(4): 1170–1183.
- Shin, U.; Lee, K.; and Kweon, I. S. 2023. Complementary Random Masking for RGB-Thermal Semantic Segmentation. *arXiv preprint arXiv:2303.17386*.
- Silberman, N.; Hoiem, D.; Kohli, P.; and Fergus, R. 2012. Indoor Segmentation and Support Inference from RGBD Images. In *European Conference on Computer Vision*.
- Tarvainen, A.; and Valpola, H. 2017. Mean teachers are better role models: Weight-averaged consistency targets improve semi-supervised deep learning results. *Advances in neural information processing systems*, 30.
- Tsai, Y.-H. H.; Bai, S.; Liang, P. P.; Kolter, J. Z.; Morency, L.-P.; and Salakhutdinov, R. 2019. Multimodal transformer for unaligned multimodal language sequences. In *Proceedings of the conference. Association for computational linguistics. Meeting*, volume 2019, 6558. NIH Public Access.
- Wang, H.; Chen, Y.; Ma, C.; Avery, J.; Hull, L.; and Carneiro, G. 2023. Multi-modal learning with missing modality via shared-specific feature modelling. In *Proceedings of the IEEE/CVF Conference on Computer Vision and Pattern Recognition*, 15878–15887.
- Wang, X.; Kumar, D.; Thome, N.; Cord, M.; and Precioso, F. 2015. Recipe recognition with large multimodal food dataset. In *2015 IEEE International Conference on Multimedia & Expo Workshops (ICMEW)*, 1–6. IEEE.
- Wang, Y.; Chen, X.; Cao, L.; Huang, W.; Sun, F.; and Wang, Y. 2022. Multimodal token fusion for vision transformers. In *Proceedings of the IEEE/CVF conference on computer vision and pattern recognition*, 12186–12195.
- Wang, Y.; Huang, W.; Sun, F.; Xu, T.; Rong, Y.; and Huang, J. 2020a. Deep multimodal fusion by channel exchanging. *Advances in neural information processing systems*, 33: 4835–4845.
- Wang, Y.; Sun, F.; Lu, M.; and Yao, A. 2020b. Learning deep multimodal feature representation with asymmetric multi-layer fusion. In *Proceedings of the 28th ACM International Conference on Multimedia*, 3902–3910.
- Wei, S.; Luo, C.; and Luo, Y. 2023. MMANet: Margin-aware distillation and modality-aware regularization for incomplete multimodal learning. In *Proceedings of the IEEE/CVF Conference on Computer Vision and Pattern Recognition*, 20039–20049.
- Woo, S.; Lee, S.; Park, Y.; Nugroho, M. A.; and Kim, C. 2023. Towards good practices for missing modality robust action recognition. In *Proceedings of the AAAI Conference on Artificial Intelligence*, volume 37, 2776–2784.
- Wortsman, M.; Ilharco, G.; Kim, J. W.; Li, M.; Kornblith, S.; Roelofs, R.; Lopes, R. G.; Hajishirzi, H.; Farhadi, A.; and Namkoong, H. 2022. Robust fine-tuning of zero-shot models. In *Proceedings of the IEEE/CVF Conference on Computer Vision and Pattern Recognition*, 7959–7971.
- Wu, R.; Wang, H.; Dayoub, F.; and Chen, H.-T. 2024. Segment Beyond View: Handling Partially Missing Modality for Audio-Visual Semantic Segmentation. In *Proceedings of the AAAI Conference on Artificial Intelligence*, volume 38, 6100–6108.
- Xie, E.; Wang, W.; Yu, Z.; Anandkumar, A.; Alvarez, J. M.; and Luo, P. 2021. SegFormer: Simple and efficient design for semantic segmentation with transformers. *Advances in neural information processing systems*, 34: 12077–12090.
- Xu, P.; Zhu, X.; and Clifton, D. A. 2023. Multimodal learning with transformers: A survey. *IEEE Transactions on Pattern Analysis and Machine Intelligence*.
- Yu, B.; Zhou, L.; Wang, L.; Frupp, J.; and Bourgeat, P. 2018. 3D cGAN based cross-modality MR image synthesis for brain tumor segmentation. In *2018 IEEE 15th International Symposium on Biomedical Imaging (ISBI 2018)*, 626–630. IEEE.
- Yu, W.; Xu, H.; Yuan, Z.; and Wu, J. 2021. Learning modality-specific representations with self-supervised multi-task learning for multimodal sentiment analysis. In *Proceedings of the AAAI conference on artificial intelligence*, volume 35, 10790–10797.
- Zadeh, A.; Chen, M.; Poria, S.; Cambria, E.; and Morency, L.-P. 2017. Tensor Fusion Network for Multimodal Sentiment Analysis. In *Proceedings of the 2017 Conference on Empirical Methods in Natural Language Processing*, 1103–1114. Association for Computational Linguistics.
- Zadeh, A.; Zellers, R.; Pincus, E.; and Morency, L.-P. 2016. Multimodal sentiment intensity analysis in videos: Facial gestures and verbal messages. *IEEE Intelligent Systems*, 31(6): 82–88.
- Zhang, J.; Liu, R.; Shi, H.; Yang, K.; Reiß, S.; Peng, K.; Fu, H.; Wang, K.; and Stiefelhausen, R. 2023. Delivering arbitrary-modal semantic segmentation. In *Proceedings of the IEEE/CVF Conference on Computer Vision and Pattern Recognition*, 1136–1147.
- Zhang, Y.; Peng, C.; Wang, Q.; Song, D.; Li, K.; and Zhou, S. K. 2024. Unified multi-modal image synthesis for missing modality imputation. *IEEE Transactions on Medical Imaging*.

Supplementary Material

MMP: Towards Robust Multi-Modal Learning with Masked Modality Projection

S1 Datasets

In this section, we provide an overview of the datasets used in our experiments. The motivation for selecting these datasets lies in their popularity and widespread usage in the field. These datasets cover a broad range of tasks, including multimodal segmentation, classification, and sentiment analysis. We utilize these datasets to include both homogeneous and heterogeneous data types, aiming to conduct a comprehensive evaluation of the effectiveness of our approach across different modality types.

MCubeS dataset (Liang et al. 2022) is a multi-modal dataset featuring four distinct input modalities: RGB, Angle of Linear Polarization (AoLP), Degree of Linear Polarization (DoLP), and Near-Infrared (NIR). The dataset is organized into three subsets: 302 sets of images for training, 96 sets of images for validation, and 102 sets of images for testing. The dataset is annotated with per-pixel labels across 20 different material classes. This detailed annotation allows for comprehensive analysis and modeling of material properties under diverse imaging conditions.

NYUDv2 dataset (Silberman et al. 2012) comprises 1,449 aligned RGB-Depth image pairs, which are divided into 795 pairs for training and 654 pairs for testing. Each image pair has a resolution of 640×480 pixels and includes detailed annotations for 40 distinct classes. For our experiments, we utilize HHA-encoded images instead of raw depth maps following recent studies (Zhang et al. 2023; Reza, Prater-Bennette, and Asif 2023).

FMB dataset (Liu et al. 2023) is a comprehensive dataset consisting of 1,500 pairs of calibrated RGB-Infrared images. The dataset is divided into 1,220 image pairs for training and 280 image pairs for testing. It covers a broad spectrum of scenes, including various lighting and weather conditions such as the Tyndall effect, rain, fog, and intense lighting. It has per-pixel ground truth annotation for 14 classes.

UPMC Food-101 dataset (Wang et al. 2015) is widely used for multimodal classification. It contains 90,704 image-text pairs, which are split into training, validation, and test sets. The dataset features annotations for 101 distinct classes, consistent with those in the ETHZ Food-101 dataset (Bossard, Guillaumin, and Van Gool 2014).

CMU-MOSI dataset (Zadeh et al. 2016) is a popular dataset for multimodal sentiment analysis. It consists of 2,199 samples, each including audio, visual, and text modalities. The dataset is split into training, validation, and test sets with 1,284, 229, and 686 samples respectively, and includes sentiment annotations for each sample.

S2 Implementation Details

We use Python¹ 3.8.18 and PyTorch² 2.1.1 for multimodal segmentation and classification, and Python 3.10.14 and Pytorch 2.4.0+cu121 for sentiment analysis task. Experiments

are conducted using two NVIDIA RTX 2080 Ti GPUs with 16G memory. The code is configured with fixed seeds to ensure the results can be replicated.

To assess missing modality performance, we provide the available modalities to the model while setting the missing modalities to zero for visual and audio data, and to empty strings for texts.

S2.1 Multimodal segmentation

We use CMNeXt (Zhang et al. 2023) as the base model for multimodal segmentation. We use their publicly available code³ to train the base model with dropout augmentation. Then we use the resulting weights to initialize our models. The learning rate is set to 6×10^{-5} and polynomial learning rate scheduler is applied with power = 0.9. The first 10 epochs are warm-up epochs and the learning rate is set to 0.1 times the original rate. We use OHEM cross-entropy loss for FMB and MCubeS datasets, and cross-entropy loss for NYUDv2 dataset. For the optimizer, we utilize AdamW (Loshchilov and Hutter 2019) with $\epsilon = 10^{-8}$ and weight decay = 0.01. We train the model with a batch size of 4 for 500 epochs on the MCubeS and NYUDv2 datasets. For the FMB dataset, we use a batch size of 2 and train for 120 epochs.

MCubeS dataset: We adopt the data pre-processing and augmentation techniques outlined in Zhang et al. (2023). The MiT-B2 backbone from Xie et al. (2021) is utilized for this dataset. For training, the input images are resized to 512×512 , while during testing, they are set to 1024×1024 . The results are reported based on single-scale performance using predicted segmentation maps at 1024×1024 .

NYUDv2 dataset: We utilize HHA-encoded images rather than raw depth maps following SA-Gate (Chen et al. 2020) and CMNeXt (Zhang et al. 2023). The preprocessed dataset can be downloaded from the SA-Gate repository⁴. Both RGB and HHA images are resized to 640×480 pixels for both training and testing. Following the recommendation in the CMNeXt paper, we employ MiT-B4 backbone from Xie et al. (2021).

FMB dataset: We follow the data pre-processing and augmentations used by Liu et al. (2023), and MiT-B3 from Xie et al. (2021) is used as the backbone. We set the input image resolution to 800×600 during both training and testing.

S2.2 Multimodal classification

UPMC Food-101 dataset: For multimodal classification task, we use ViLT (Kim, Son, and Kim 2021) as our base model. We set the learning rate to 10^{-5} , and polynomial learning rate scheduler is applied with power = 0.9, ratio = 0.1, and the first 2500 steps as the warm-up. We use cross-entropy loss, and AdamW optimizer with a weight decay of

¹<https://www.python.org/>

²<https://pytorch.org/>

³<https://github.com/jamycheung/DELIVER/>

⁴https://github.com/charlesCXX/RGBD_Semantic_Segmentation_PyTorch/

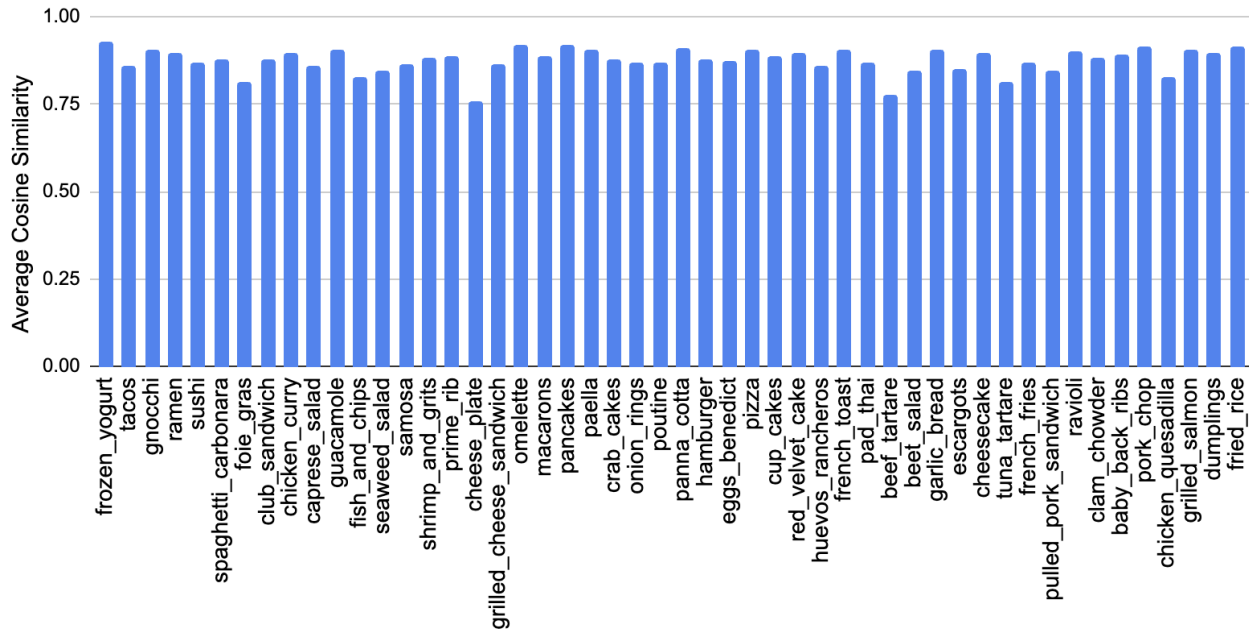


Figure S1: Average cosine similarity between model predictions with real and projected tokens on UPMC Food-101 dataset when image is missing. We substitute the missing modality tokens with the projected tokens.

0.02. Batch size is 16, and we train the model for 20 epochs. The remaining configurations for this task are the same as Lee et al. (2023).

S2.3 Multimodal sentiment analysis

CMU-MOSI dataset: For multimodal sentiment analysis, we use multimodal transformer (Tsai et al. 2019) from this publicly available code⁵, and use the default configurations from Yu et al. (2021).

S2.4 Reproducibility Statement

We made our source code and pretrained models available at this anonymous link⁶ to ensure the reproducibility of our results, and to facilitate the community in building upon our work. A comprehensive README.md file is added containing detailed instructions to set up environment, execute code, and reproduce the results. The main experimental results presented in this paper can be reproduced using the provided scripts, pretrained model weights, and instructions.

S3 Projected and Real Tokens Alignment

In this section, we examine the alignment between the real tokens of a modality and the projected tokens generated from the available modalities using our MMP approach. The alignment of these tokens is crucial. This ensures that the model can effectively predict and substitute the missing modality tokens from the available modalities. We employed a smooth L1 loss to align the projected tokens with

the real tokens during training as described in Section 3.4. This alignment loss minimizes the discrepancy between the projected tokens and the original tokens. To evaluate the effectiveness of this alignment, we employ cosine similarity for multimodal classification on the UPMC Food-101 dataset and Mean Squared Error (MSE) for multimodal sentiment analysis on the CMU-MOSI dataset. These metrics help us visualize the degree to which the model’s predictions align when using real tokens versus projected tokens during testing.

S3.1 UPMC Food-101 dataset

The first analysis is conducted on the UPMC Food-101 dataset, as illustrated in Figures S1 and S2. These figures show the cosine similarity between the model’s predictions using real tokens and projected tokens during testing. We show the cosine similarity of the first 50 out of 101 classes. Figure S1 visualizes the scenario where the image modality is missing, and its tokens are replaced with projected tokens generated from the available text modality. The results show high cosine similarity, with all similarity scores exceeding 0.75 and most classes achieving scores above 0.8.

Similarly, Figure S2 shows the cosine similarity when the text modality is missing. We see similar pattern here, with scores consistently above 0.7 and mostly above 0.8. This indicates that the MMP approach effectively projects the available modality tokens to estimate the missing ones, aligning these tokens in a manner that ensures stability in the model’s predictions.

⁵<https://github.com/thuiar/MMSA/>

⁶<https://drive.google.com/drive/folders/155IsgLD88-Dt6Q9DJCKCENuDF7vjI9Jl>

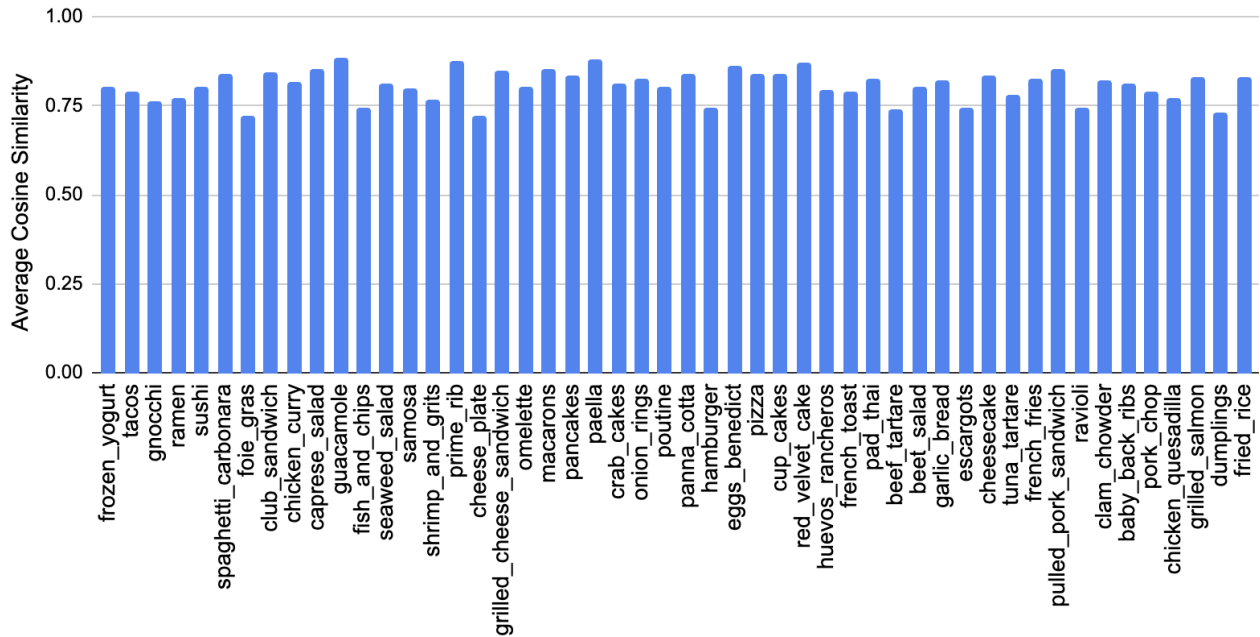


Figure S2: Average cosine similarity between model predictions with real and projected tokens on UPMC Food-101 dataset when text is missing. We substitute the missing modality tokens with the projected tokens.

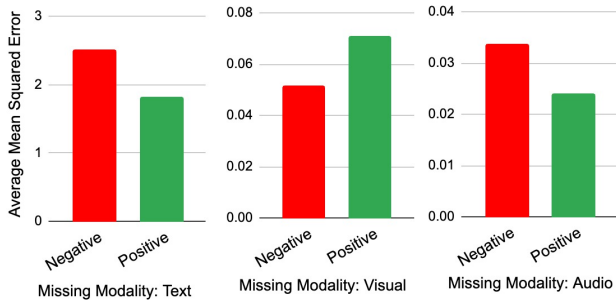


Figure S3: Average Mean Squared Error (MSE) between model predictions with real and projected tokens on CMU-MOSI dataset.

S3.2 CMU-MOSI dataset

We extend this analysis to the CMU-MOSI dataset. Figure S3 illustrates the average Mean Squared Error (MSE) for each modality. The results show that the audio modality exhibits the lowest MSE, reflecting the highest alignment between real and projected tokens. This is followed by the visual modality, which also demonstrates low MSE. The text modality shows a higher MSE, though it remains below 3. This observation is consistent with related work, which has shown that the text modality often has the most significant impact when missing, making it more challenging to project accurately.

S4 Evaluation Metrics

In this section, we describe the evaluation metrics used to assess the performance of our MMP approach across three different tasks. We utilize mean Intersection over Union

(mIoU) for segmentation, accuracy for classification, and binary accuracy and F1-score for sentiment analysis. These metrics are standard in their respective fields, and it is common practice to use them for benchmarking against related work.

S4.1 Multimodal Segmentation

For the multimodal segmentation task, we use the mean Intersection over Union (mIoU) as the evaluation metric. mIoU is a standard metric for evaluating semantic segmentation performance. It calculates the average overlap between the predicted segmentation and the ground truth across all classes. This provides a comprehensive evaluation by considering both false positives and false negatives, and capturing the spatial overlap between the predicted and true segmentations.

S4.2 Multimodal Classification

For the multimodal classification task, we employ accuracy as our evaluation metric. Accuracy measures the proportion of correct predictions made by the model out of all predictions. This is a straightforward and intuitive metric that provides an overall performance measure of the classification model.

S4.3 Multimodal Sentiment Analysis

For the multimodal sentiment analysis task, we utilize both accuracy and F1-score to evaluate the model's performance. F1-score is the mean of precision and recall, providing a balance between the two. We use the binary metrics in this task, which only consider the Negative and Positive classes, following the common approach in related work.